Oil Spill Contingency and Response Modelling in Ice-Covered Waters

Tor Nordam*, Emma Litzler, Petter Rønningen, Joakim Aune, Thomas F. Hagelien,
Arve Loktu, CJ Beegle-Krause, Ute Brönner
SINTEF Ocean
Trondheim, Norway
*tor.nordam@sintef.no

Abstract

This paper describes several updates to SINTEF's Oil Spill Contingency and Response (OSCAR) model, which have significantly improved the modelling of oil spills in cold and ice-covered waters. In addition to transport of surface oil with ice velocity from an external ice model, OSCAR can now calculate vertical mixing from a combination of velocity shear and stratification, or read diffusivity data from netCDF files. Calculation of the wave field in the vicinity of ice is more realistic, and OSCAR can also predict the ignitability of surface oil. All of these improvements are of particular importance in the cold regions.

Taking the effect of stratification on vertical mixing into account is particularly important in the Arctic, as brine rejection during freeze-up can give a very deep mixed layer, while freshwater from melting ice can give a strong, shallow pycnocline. The wave contribution to vertical mixing is reduced in the presence of ice, and dynamic ice cover is also taken into account in the fetch length for calculating the wave field in open water close to the ice.

Finally, the calculation of ignitability for surface oil will give a prediction of the window of opportunity for *in-situ* burning as a response option. The ignitability calculation builds on earlier experimental work done at SINTEF, and uses a calibrated statistical model to predict (for each location with surface oil) whether the surface oil is ignitable, based on weathering state, water content, viscosity, asphaltene content and wax content. The window of opportunity for *in-situ* burning will, in many cases, be longer in cold and ice-covered regions, due to reduced evaporation and emulsification. Hence, the ability to calculate ignitability is highly relevant for contingency planning and environmental risk assessment in the Arctic.

1 Introduction

Oil spill modelling is the go-to approach when it comes to planning of contingency and response options in the case of accidental discharges during exploration drilling or the production phase of an oil field. Oil spill models need to account for oil transport in the near- and far-field of the release, as well as different processes affecting the properties of the oil, such as oil weathering or chemical treatment, in order to calculate fate. These processes are often implemented as sub-models to the main trajectory model and several sub-models are usually combined for a given scenario.

Applying oil spill modelling in ice-covered waters makes it necessary to include the effects of ice into these sub-models. Ice will affect transport by damping waves and changing vertical mixing, and it will modify the effect of wind on the currents near the ice-water interface. The presence of ice will also directly and indirectly affect oil weathering due to lower temperatures, less wave energy and reduced evaporation due to smaller area of open water.

This paper describes recent work that was done to adapt processes in SINTEF's Oil Spill Contingency And Response (OSCAR) model to make the model more fit for the purpose of environmental risk assessment and contingency planning in areas with ice-covered waters. In this introduction, a background on the modelling of oil spills in ice is given, as well as some background on the OSCAR model, and SINMOD, which was the coupled ice-ocean model used to produce ice and ocean data for the case studies. In Section 2, the improvements

Nordam, T., E. Litzler, P. Ronningen, J. Aune, T.F. Hagelien, A. Luktu, C.J. Beegle-Krause, and U. Bronner, Oil Spill Contingency and Response Modelling in Ice-covered Waters, Proceedings of the Forty-first AMOP Technical Seminar, Environment and Climate Change Canada, Ottawa, ON, Canada, pp. 957-973, 2018.

made to OSCAR are described in detail, and in Section 3, we demonstrate the new features by presenting the results of some selected case studies. Finally, in Section 4, we summarise the results of this work.

1.1 Oil Spill Modelling in Ice-Covered Waters

For the movement of surface oil in ice covered waters, there exists a general rule of thumb initiated in the 1970s, describing a transition between how ice moves in lower ice concentrations as compared to heavy ice conditions. The concept is that the oil moves with the winds and currents, as in open water, at less than 30% ice cover, and that ice controls the oil movement completely above 70% - 80% ice cover. El-Tahan et al. (1988) first published this rule of thumb. Later, Venkatesh et al. (1990) discussed and analysed these limits, and presented a theoretical argument for the upper limit based on the fact that at 80% coverage, circular ice floes would be packed so close that they would almost all be touching their neighbours, leaving little or no space for the oil to move past. The behaviour at intermediate ice covers between 30% and 70% - 80% has been assumed to be a linear transition from one regime to the other, as no field calibration has been done.

In addition to modifying transport, the presence of ice will leave less open water surface, which will increase the thickness of the oil, and give a smaller area available for evaporation of light oil components. As well as affecting the oil through direct contact, the presence of ice will also influence the water column. Ice freezing leads to brine rejection, which destabilises the upper water column, leading to overturning, increased vertical mixing and further heat loss to the atmosphere. During the melting season, the increased stratification due to freshwater overlaying oceanic water gives a stable upper water column, reducing vertical mixing.

As a part of the recent JIP on Arctic Response Technology (for further details, see www.arcticresponsetechnology.org) the OSCAR model was advanced to read ice data, including ice coverage and velocity, from the standard netCDF format, and transport of surface oil with the externally calculated ice velocity was implemented (Nordam et al., 2018). In the work presented here, we build on this foundation to further improve modelling of oil in ice-covered waters with OSCAR.

1.2 The OSCAR Oil Spill Model

OSCAR is a state-of-the-art oil spill trajectory, fate, effects and response model that has been continuously developed and applied to oil spill contingency planning and environmental risk assessment for several decades (Reed et al., 2000). OSCAR is fully 3D, and accounts for processes in the four compartments sea surface, water column, shoreline and sea floor. OSCAR includes oil weathering, the physical and chemical processes that affect and change oil at sea, such as biodegradation, emulsification, and evaporation. The development of sub-models for these processes has been strongly coupled with laboratory and field activities at SINTEF, including small-scale testing of weathering properties, meso-scale experiments studying blowouts and sub-sea dispersant injection in the SINTEF tower basin, as well as full-scale field tests (Brandvik et al., 2013; Johansen et al., 2013; 2015; 2003).

At the sea surface, OSCAR computes surface oil spreading, slick transport, entrainment into the water column, shore interactions, and weathering processes (e.g. evaporation, biodegradation, and emulsification). In the water column the model will account for horizontal and vertical transport by currents, dissolution, adsorption, settling and biodegradation. Changes in composition due to evaporation, dissolution and biodegradation will alter the physical properties of the oil, including density, viscosity, solubility, volatility, and the aquatic

toxicity of the dissolved oil fraction. In order to accurately model these effects, OSCAR represents oil in terms of 25 pseudo-components (Reed et al., 2000). These components represent hydrocarbon groups with similar physical and chemical properties. Biodegradation is computed per pseudo-component with respective rates for each component for the dissolved phase, the droplet phase, surface oil and oil in the sediments.

OSCAR uses a Lagrangian particle transport model, where the release is represented by numerical particles (also known as Lagrangian elements, or "spillets") for the dissolved, droplet and gas fractions of the release. Each numerical particle is tracked through a flow field, calculated from currents, wind, and ice (if present). Mixing due to unresolved turbulent motion is implemented as a random component in the horizontal and vertical displacement of the particles, where the step length of the random walk is calculated from the diffusivity. Vertical mixing is discussed in more detail in Section 2.2.

Each numerical particle holds information about its position (longitude, latitude, depth), size (radius of a disk if surfaced, radius and height of a cylinder if submerged) and the mass of each of the 25 pseudo-components (Reed et al., 2000). When aggregate quantities such as surface oil thickness, or concentration of dissolved components, are calculated, the particles are projected onto a grid in two or three dimensions. Some further details on the grid projection are given in Section 2.3

1.3 The SINMOD Hydrodynamic Model

Oil spill models need environmental data to describe the ambient conditions surrounding the released oil. In OSCAR these data include time-varying 3D fields for currents, and time-varying 2D fields for wind, ice coverage and ice velocity. Optionally, one can also use time-varying 3D fields for temperature, salinity and dissolved oxygen. Temperature and salinity are used to calculate the density of seawater, which is required to take stratification into account in the vertical mixing. In the case studies presented in Section 3, the oceanographic data used as input to OSCAR were created by the SINMOD hydrodynamic and biological model (Slagstad and McClimans, 2005).

SINMOD has been developed at SINTEF for the modelling of ocean circulation and marine resources, and contains a module for marine ecosystems at the lower trophic levels, in addition to a coupled ice-ocean model. The hydrodynamic module used in SINMOD is based on the primitive Navier-Stokes equations and is established on a z-grid (constant-depth discretisation). A vertical turbulent mixing coefficient is calculated as a function of the Richardson number, Ri, in the water column (Sundfjord et al., 2008), and from the wave state near the surface (Ichiye, 1967). Waves are calculated from wind speed and fetch length. Horizontal mixing is calculated according to Smagorinsky (1963).

The ice model in SINMOD is a Hibler-type formulation (Hibler III, 1979), and has two state variables: the average ice thickness in a grid cell, h, and the fraction of a grid cell covered by ice, A. The remaining fraction, $1 - A$, is open water. The equation solver uses the elastic-viscous-plastic mechanism as described by Hunke and Dukowicz (1997).

The SINMOD model area used to generate the hydrodynamic data for this study covers the area around Greenland, and is shown in blue outline in Fig. 1. The model area has a spatial resolution of 4 km $\times$ 4 km, and the dataset produced has a temporal resolution of 1 hour. Boundary conditions were taken from a larger model domain, at 12 km $\times$ 12 km resolution. A total of 8 tidal components were imposed by specifying the various components at the open boundaries of the large-scale model. Tidal data were taken from the TPXO 6.2 model of global ocean tides (Egbert et al., 1994). Atmospheric data from the ERA-Interim Reanalysis (Dee et al., 2011) have been used to force the ocean model.

Figure 1 Map showing the outline of the SINMOD model domain used to produce data for the case studies in this paper.

2 Updated Sub-Models in OSCAR

When ice is present, the modelling of surface and near-surface oil is modified in several ways as compared to open water. Surface oil in partial ice cover resides between the ice floes, which means there is less surface available for evaporation, and that the oil becomes thicker. Lower temperatures will also contribute to less evaporation, and within a given area, biodegradation is generally slower in cold temperatures during winter, as compared to warm temperatures in summer (Bagi et al., 2013; Lofthus et al., 2018). This will have the effect of slowing weathering processes. Additionally, waves are damped, which will reduce the rate of entrainment and water uptake into the emulsion. The damping of waves also means there is less vertical mixing in the water column near the surface.

In this section, we describe the modification and implementation in OSCAR of sub-models that are relevant in cold or ice-covered waters, either because they directly include ice, or because they involve phenomena expected to be particularly relevant in cold regions.

2.1 Oil Transport with Ice

Windage is the effect that wind has on the movement of surface oil. This is generally considered to be somewhere in the range of 0% to 6% (see e.g. ASCE (1996); Beegle-Krause (2018)), with a common value being 3% (Simecek-Beatty, 2011), which means that oil at the surface is assumed to move with the velocity of the water, plus 3% of the velocity of the wind:

$$\mathbf{v}_{oil} = \mathbf{v}(z = 0) + 0.03 \cdot \mathbf{u}_{10}, \tag{1}$$

where $\mathbf{v}(z = 0)$ is the velocity of the water at the surface, and $\mathbf{u}_{10}$ is the wind velocity. The wind velocity is assumed to be given at 10 meters above the ocean surface, which is a standard convention. When ice is present, it will modify the transport of oil at or near the sea surface. Ice affects the windage of the oil, and in addition, the ice itself will move with the winds

and currents. A coupled ice-ocean hydrodynamic model will typically predict not only ice coverage and thickness, but also the velocity of the ice. When this information is available, it can be used to calculate the movement of oil at or near the surface in full or partial ice cover.

The transport of surface oil takes the ice velocity into account when relevant. If ice coverage is less than 30%, the transport is as in open water, i.e. given by Eq. (1). If the ice coverage is above 80%, surface oil moves with the ice velocity. If ice coverage is between 30% and 80%, a linear transition between the two extremes is used. Note that the term "surface oil" here refers to both oil at the sea surface, and oil trapped at the ice-water interface (i.e. oil at a depth of 0 m). For further details on the implementation in OSCAR, see Nordam et al. (2018).

If ice coverage is available in the input data, but not ice velocity, OSCAR will estimate the ice velocity by

$$\mathbf{v}_{ice} = \mathbf{v}(z = 0) + 0.015 \cdot \mathbf{u}_{10}, \tag{2}$$

where $\mathbf{v}(z = 0)$ is the velocity of the water at the surface, and $\mathbf{u}_{10}$ is the wind velocity (Reed and Aamo, 1994). This simple rule of thumb does not take into account the rheology of the ice, i.e., the fact that the ice in a grid cell is subjected to forces from ice in the neighbouring grid cells. The rheology of the ice will be taken into account by a coupled ice-ocean model. Hence, ice velocity from such an ice-ocean model should be used whenever available, as it is expected to be more accurate than that predicted from a simple heuristic, such as Eq. (2).

2.2 Vertical Mixing

Vertical mixing is caused by turbulence, which has several origins: waves, friction against sea ice and sea bed, current shear in the free water masses, etc. However, vertical mixing is also inhibited by stable density gradients. A sharp increase in density with depth will strongly inhibit vertical mixing, as energy is required to lift dense water up, and push light water down. For this reason, density gradients should be taken into account in calculating the vertical mixing. State-of-the-art ocean models include simulation of temperature and salinity, and making these fields available to the trajectory model allows the density of the water to be calculated.

Vertical mixing is implemented as a random walk process in OSCAR, where the step length in the random walk is calculated from a diffusivity profile, $K_v(z)$, which gives the diffusivity as a function of depth at a given location. The vertical diffusivity profile, $K_v(z)$, is the sum of a contribution from waves, $K_w(z)$, and a contribution from the current shear and stratification, $K_{vm}(z)$, and is given by

$$K_v(z) = K_w(z) + K_{vm}(z), \tag{3}$$

where $K_w(z)$ is given by Eq. (4), and $K_{vm}(z)$ is given by Eq. (6).

In addition to calculating diffusivity, OSCAR has the option to read time-resolved 3D horizontal and/or vertical diffusivity fields from an external source, via netCDF files. These can for example be provided from an ocean model, or a special purpose turbulence model, or even from measured profiles if available.

2.2.1 Vertical Mixing from Waves

Vertical mixing due to waves is calculated in OSCAR from wave height and wave period according to Ichiye (1967):

$$K_w(z) = 0.028 \frac{H_s^2}{T_p} \mathrm{e}^{-2kz}. \tag{4}$$

Here, z is the depth at which the mixing is calculated (depth positive downwards). The wave parameters H_s and T_p are the significant wave height and the peak wave period, and k is the wave number, which is found from the peak period by the dispersion relation for deep water waves, $\omega^2 = gk$, where the angular frequency is given by $\omega = 2\pi/T_p$ (see e.g. Stewart (2008)). H_s and T_p are derived from the JONSWAP spectrum and associated empirical relations (Carter, 1982). The sea state is assumed to be either fully developed, or fetch-limited. Fully developed here refers to the steady-state wave conditions which are reached very far away from land or sea ice, when the wind remains constant for a long time. Fetch-limited refers to the steady-state that is reached when the fetch is too short to allow the sea to reach the fully developed state. In both cases, the wind is assumed to have been constant for sufficient time that the wave spectrum is not time-limited (i.e., a steady state is assumed to have been reached).

H_s and T_p are given by

$$H_s = \frac{u_{10}^2}{g} H_c \sqrt{\frac{gL_f}{u_{10}^2}} \tag{5a}$$

$$T_p = \frac{u_{10}}{g} T_c \sqrt[3]{\frac{gL_f}{u_{10}^2}} \tag{5b}$$

in the fetch-limited case, and

$$H_s = \frac{u_{10}^2}{g} H_0 \tag{5c}$$

$$T_p = \frac{u_{10}}{g} T_0 \tag{5d}$$

in the fully developed case. Here, $H_0 = 0.243$, $H_c = 0.0016$, $T_0 = 8.134$, and $T_c = 0.286$ are dimensionless parameters, g is the gravitational acceleration, L_f is the fetch length, and u_{10} is the wind speed at 10 m above sea level. Additionally, the peak period has a depth-dependent upper limit of

$$T_p = T_{max} \sqrt{\frac{d}{g}}, \tag{5e}$$

which acts as a limit in shallow waters (Rye et al., 2006; US Army Corps Of Engineers, 1984). Here, d is the water depth, and $T_{max} = 9.78$ s^{-1}.

The fetch length is the distance over which the wind acts to create waves before reaching a given position. For each location in the model area, the fetch is calculated as the distance to the closest land or high ice cover in the upwind direction, as shown in Fig. 2. In previous versions of OSCAR, only the upwind distance to nearest land was used, but as waves will not form in areas of high ice cover, the upwind distance to the ice edge should be used when ice is present. A limit of 80% ice cover has been chosen to define the ice edge for this purpose.

As the ice cover is changing with time throughout a simulation, this necessitates the recalculation of the fetch at each location each time the ice cover changes. Whenever the ice coverage changes, a fetch grid is calculated for each of the four cardinal directions North, East, South and West. For each direction, the fetch on the border of the grid is set to 100 km for open sea and 0 km for cells over land or areas with high ice cover. The rest of the grid is

Nordam, T., E. Litzler, P. Ronningen, J. Aune, T.F. Hagelien, A. Luktu, C.J. Beegle-Krause, and U. Bronner, Oil Spill Contingency and Response Modelling in Ice-covered Waters, Proceedings of the Forty-first AMOP Technical Seminar, Environment and Climate Change Canada, Ottawa, ON, Canada, pp. 957-973, 2018.

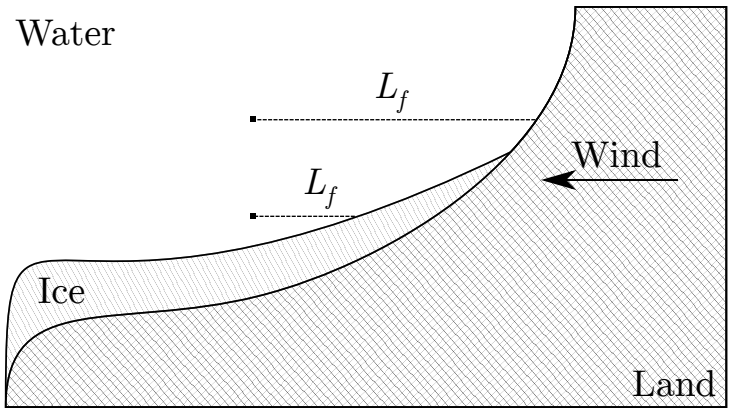

Figure 2 When high ice cover is present, fetch should be calculated as the upwind distance to the nearest ice edge or land, whichever is closer. Here we use an ice cover of 80% to define the ice edge.

then deduced moving downwind. In calculating the wave field, the waves at each location are calculated from the wind speed and direction at that point, using the fetch calculated for the closest cardinal direction.

2.2.2 Vertical Mixing from Velocity Shear and Stratification

OSCAR now has the option of dynamically calculating a contribution to the vertical diffusivity from the hydrodynamic input data, if time- and depth-resolved temperature and salinity fields are available (in addition to ocean current data). The scheme used is the same as that in the SINMOD ocean model (Sundfjord et al., 2008), although it can be used with data from any ocean model as long as the required variables are available. The contribution to the vertical diffusivity calculated from current shear and stratification is given by:

$$K_{vm} = K_{vm_0}\left(\frac{\arctan\left(G\left(\mathrm{Ri}_0 - \mathrm{Ri}\right)\right)}{\pi} + \frac{1}{2}\right) \tag{6}$$

where $K_{vm_0} = 3 \times 10^{-2}\,\mathrm{m}^2/\mathrm{s}$, $G = 30$, and $\mathrm{Ri}_0 = 0.65$. The Richardson number, Ri, is a dimensionless number describing the relative importance of velocity shear and density gradients, given by:

$$\mathrm{Ri} = \frac{g}{\rho}\frac{\partial\rho/\partial z}{\left(\partial\mathbf{v}/\partial z\right)^2}. \tag{7}$$

Here, ρ is the density of seawater (in OSCAR, this is calculated from temperature and salinity according to Millero and Poisson (1981)), and

$$\left(\frac{\partial\mathbf{v}}{\partial z}\right)^2 = \left(\frac{\partial u}{\partial z}\right)^2 + \left(\frac{\partial v}{\partial z}\right)^2, \tag{8}$$

where u and v are respectively the east and north components of the current vector $\mathbf{v}$. Large values of Ri indicate that turbulent mixing by current shear is suppressed by stable density gradients.

In Fig. 3, an example of a calculation of diffusivity from hydrodynamic data is shown. Density is calculated from temperature and salinity, which are provided by the hydrodynamic model. The derivatives with respect to z in Eqs. (7) and (8) are calculated with central finite differences at the interior grid points, and one-sided finite differences at the endpoints. Interpolation is used to evaluate the diffusivity between gridpoints.

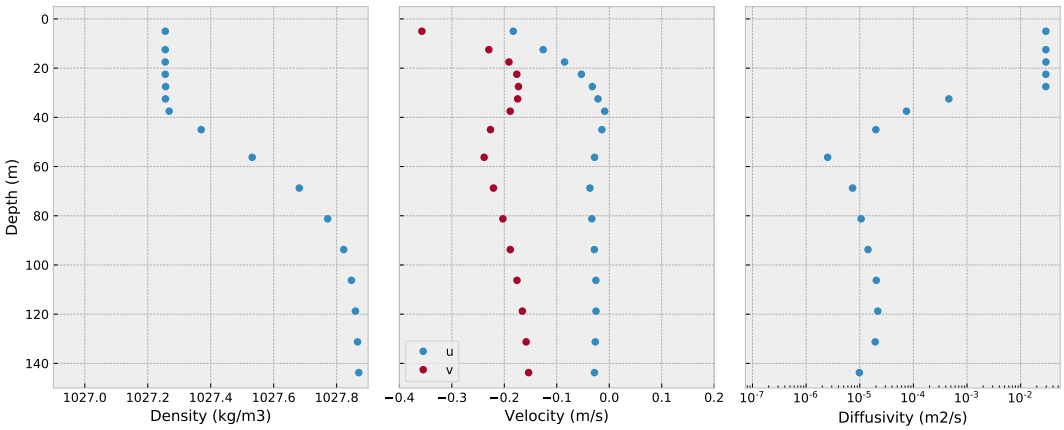

Figure 3 To the left, density (calculated from modelled temperature and salinity), in the middle, modelled horizontal current velocity components, and to the right diffusivity calculated from Eq. (6) (thus not taking waves into account). The diffusivity is calculated for each grid point in the depth profile, and interpolation is used to evaluate the diffusivity between grid points.

2.3 Window of Opportunity for *in-situ* Burning

In order for *in-situ* burning to be available as a response option, several conditions must be met. In addition to operational constraints related to the weather, the oil must have enough light components to be ignitable, the water content must not be too high, and the oil slick must be sufficiently thick. If the oil is too thin, the heat loss to the water will be too large to sustain a burn. For this reason (as well as reasons of safety), a fire boom or other mechanical barrier is usually used to contain the oil in a smaller area during a burn.

OSCAR now includes the ability to calculate the ignitability of surface oil. It should be noted that this calculation does not take the thickness of the oil into account, but rather calculates if the oil is in an *ignitable state*. If the oil is in an ignitable state, then *in-situ* burning should be possible, provided the oil can be concentrated to sufficient thickness by fire booms or similar.

The calculation of ignitability is based on earlier experimental work at SINTEF. A large number of samples were prepared from five different oils, at different weathering degrees and with different water content (see Table 1). These samples were then characterised by measuring a range of different properties, and tested to see if they could be ignited. Finally, statistical analysis was used to identify the most important parameters for predicting ignitability, and to create an empirical model. This model takes the form of an equation (Eq. (11a)) and a set of coefficients (Eq. (11b)) that predict ignitability as a function of

- water content,
- asphaltene content,
- wax content,
- flash point of water-free oil,
- shear viscosity.

A more complete description of this work is found in Brandvik et al. (2010). The required parameters for calculating ignitability are calculated by OSCAR for each individual numerical particle, and will depend on the age and history of that particle. Emulsification is calculated based on the properties of the oil and the sea state, and water content will increase as the oil

Oil type	*Residue*	*Density (Kg/L)*	*Evap loss (Vol.%)*	*Pour point (°C)*	*Wax (wt.%)*	*Asphaltenes (wt.%)*
Troll B	Fresh	0.900	0	-36	0.9	0.04
	250°C	0.930	25.5	-27		
Norne	Fresh	0.860	0	21	10.8	0.3
	250°C	0.888	28.4	30		
Kobbe	Fresh	0.797	0	-39	3.4	0.03
	250°C	0.875	53.6	21		
Statfjord	Fresh	0.835	0	-6	4.3	0.1
	250°C	0.896	42.4	21		
Grane	Fresh	0.941	0	-24	3.2	1.4
	250°C	0.968	13	-6		

Table 1 Physical and chemical properties of the oils used in the experiments. Note that wax and asphaltene content is here given in percent.

forms a water-in-oil emulsion on the sea surface. Asphaltene and wax content are both calculated from the initial composition of the oil and the degree of evaporation, and will increase with time as lighter oil components are lost to evaporation. In this calculation, we assume that wax and asphaltenes do not evaporate, and scale the asphaltene and wax contents by the evaporated fraction:

$$f_w = \frac{f_{w0}}{1 - f_e}, \tag{9}$$

where f_w is the calculated wax fraction, f_{w0} is the initial wax fraction of the oil, and f_e is the fraction of the oil mass that has evaporated. The calculation for asphaltenes is identical, but using f_{a0}, the initial asphaltene fraction of the oil.

Flash point of the water-free oil is calculated by curve-fit of experimental data. As part of the weathering study of an oil, the flash point is measured at different weathering degrees (i.e., different evaporated fractions). The logarithm of the flash point has been observed to be reasonably well approximated by a linear function of evaporated fraction (Johansen, 1991). This is used to calculate flash point as a function of degree of evaporation.

Shear viscosity is also calculated by scaling of experimentally measured values. This is done in a two-step process, where first a viscosity is calculated for the water free oil, based on the evaporated fraction, and then that value is used as a starting point to calculate the viscosity of the emulsion, based on the water content (Daling et al., 1990).

Prior to calculation of ignitability, a projection from spillets to a surface grid is done. As surface spillets are modelled as disks (cylinders if submerged), a spillet can contribute to one or more cells in the surface grid. For a spillet i, its mass, m_i, is distributed over the cells overlapping with that spillet. For each cell in the surface grid, the mass of the emulsion in that cell, M, is given by:

$$M = \sum_i \frac{m_i}{N_i}, \tag{10}$$

where N_i is the number of cells with which spillet i overlaps. The values of the different parameters in the calculation of the ignitability are then calculated for each cell as mass-weighted averages of the contribution from each spillet overlapping that cell.

The empirically derived equation for ignitability (Brandvik et al., 2010) is

$$I = A_1 + A_2 f_{\mathrm{H_2O}} + A_3 f_a + A_4 T_f + \left(A_5 + A_6 f_{\mathrm{H_2O}}\right) \log_{10}(\mu) + \left(A_7 f_{\mathrm{H_2O}} + A_8 f_a\right) f_w \tag{11a}$$

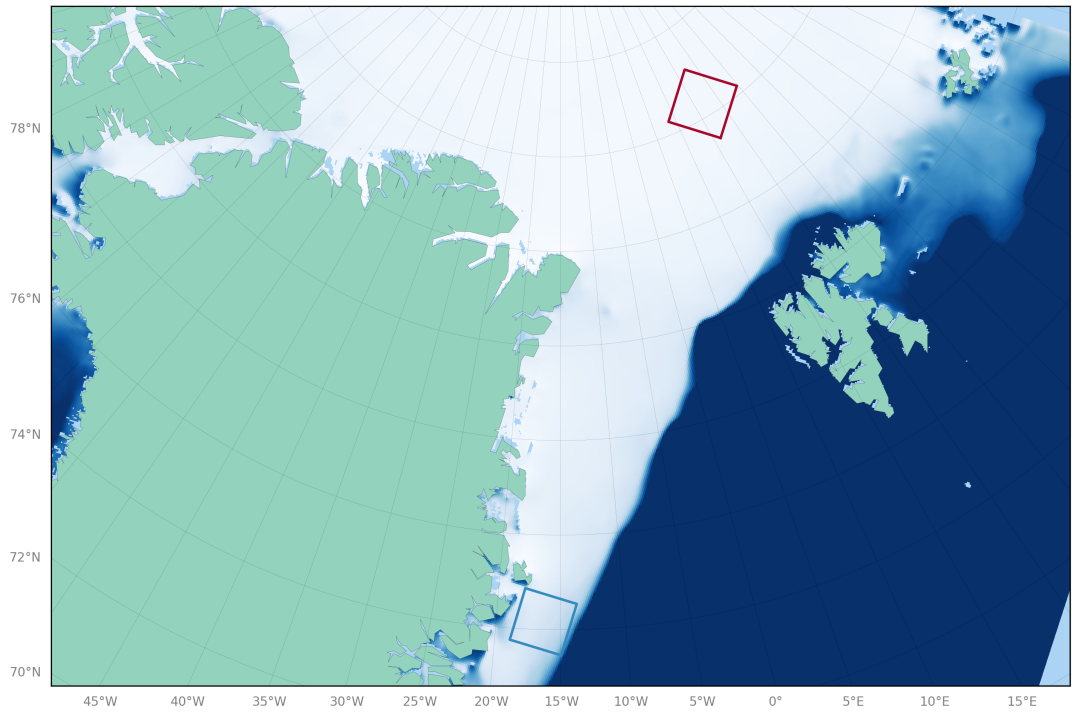

Figure 4 Map showing the two locations selected for the case study. The two squares are 120 km × 120 km, and the simulated release points were placed in the middle of each square. Data for January 1, 2007, was used.

where f_{H_2O}, f_a and f_w is the water content, asphaltene content and wax content (mass fraction), T_f is the flash point of the water free oil (°C), and μ is the shear viscosity of the oil (cP). The coefficients A_i are:

$$\begin{aligned} A_1 &= 0.8003, & A_2 &= 1.185, \\ A_3 &= 27.6719, & A_4 &= -0.0035, \\ A_5 &= 0.14691, & A_6 &= -0.6087, \\ A_7 &= -0.0699, & A_8 &= -9.6274. \end{aligned} \tag{11b}$$

A_4, A_5 and A_6 have the appropriate units such that I is dimensionless. This formula gives a binary prediction: if $I \leq 0.5$, the oil is not ignitable, and if $I > 0.5$, it is.

In the experimental work on which Eqs. (11) are based, the five different oil types described in Table 1 where used. These were chosen to span a wide range of properties. The properties of different oils are taken into account mainly through the parameters asphaltene content, wax content and flash point. It is expected that the calculation of ignitability should be applicable to any oil, as long as its properties are not too far outside the range spanned by the five oils on which the equation is based.

3 Results and Case Studies

In this section, we present the results of some case studies that have been selected to demonstrate the effect of the new improvements to OSCAR.

3.1 Vertical Mixing

The effect of including stratification in the calculation of the vertical mixing is expected to be important in many cases. As an example, we have here considered a fictional

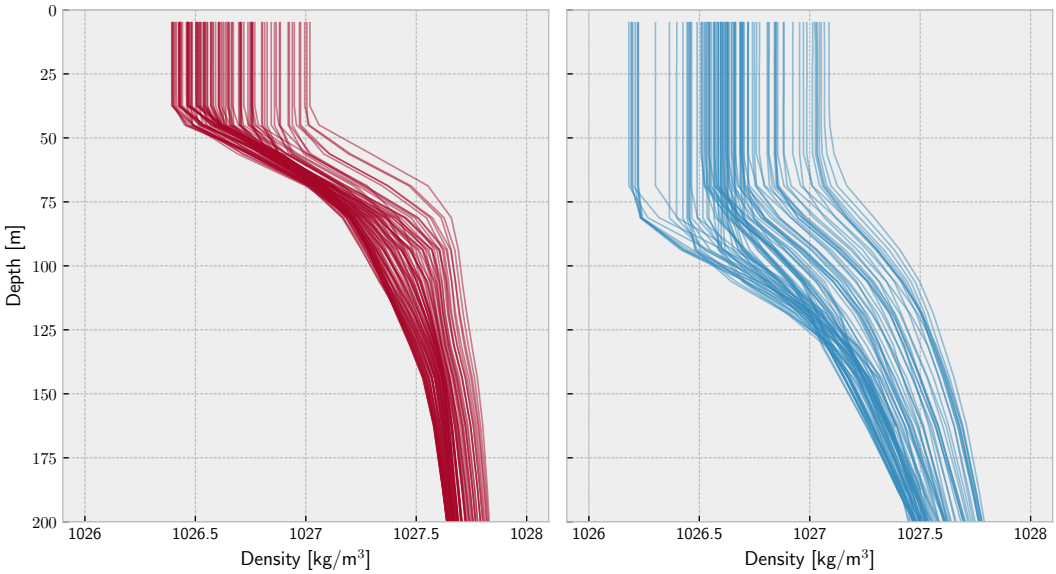

Figure 5 Density profiles based on modelled temperature and salinity from the two different locations shown on the map in Fig. 4. 100 profiles at evenly spaced points are shown for each of the two regions, with values for each vertical layer positioned at the midpoint of the layer. The northern of the two regions is shown to the left.

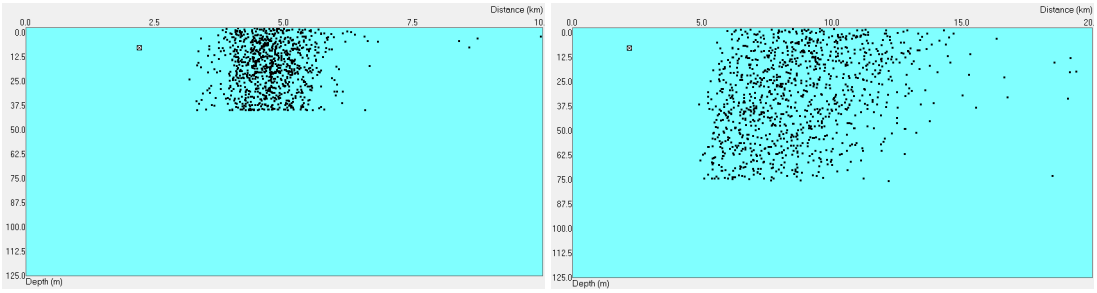

Figure 6 Distribution of oil droplets in the water column, for an idealised case where small droplets are released into the water column at a depth of 5 m. The northern of the two locations outlined in Fig. 4 is shown to the left.

case where small oil droplets (between 20 and 200 micrometers) are released into the water column from a depth of 5 meters. This idealised scenario has been selected in order to highlight the effect of vertical mixing, and is intended to mimic a situation where surface oil has been treated with dispersants and mixed down by applied energy (such as propwash from a response vessel). This has been modelled at two different locations, with different stratification, which in turn leads to different mixing. The two locations are shown on the map in Fig. 4. In one case, the pycnocline is at a depth of about 40-50 meters, while in the other case it is at about 70-90 meters depth. Density profiles for the two cases are shown in Fig. 5 (the value in each layer is shown at the midpoint of that layer). In both cases, the density is constant in the upper part of the water column, indicating the presence of a well mixed layer.

In Fig. 6, a vertical cross section showing the distribution of oil droplets after 24 hours is shown. In both cases, the smaller oil droplets are distributed throughout the mixed layer. The differences in vertical distribution in turn lead to differences in the time for the oil to surface. In the northern location, the oil is mixed down to about 40 meters, and about 59%

of the oil has surfaced (i.e., reached the ice-ocean interface) after 24 hours. In the southern location, the mixed layer has a depth of about 80 meters, and only 53% of the oil has surfaced.

In both of these cases there is high ice cover, which removes any mixing due to waves. The difference in mixing depth in the two cases is thus mainly due to the different density profiles in the water column, as well as any differences in current shear (see Eq. (6)).

3.2 Fetch

To demonstrate the effect of taking ice cover into account in the calculation of fetch, we have considered a fictional case where we simulate a well blowout near the Marginal Ice Zone (MIZ) in the Barents Sea (see Fig. 7). The oil is surfacing in open water, just to the south of the ice. At the start of the simulation, the wind direction is from the south and towards the ice, moving the oil into the MIZ. At this time, the wave state is fully developed. After about 6 days, the wind picks up, and changes to the off-ice direction.

When simulating this without taking the ice cover into account in the fetch length, a large fraction of the surface oil is rapidly mixed down into the water column when the wind picks up towards the south on day 6. When the ice cover is taken into account, on the other hand, the wave state becomes fetch-limited, due to the short distance to the ice in the upwind direction. As a consequence, the amount of oil that gets submerged is substantially lower. In Fig. 8, the amount of oil at the surface is shown as a fraction of the total amount of oil at the surface and in the water column, along with the direction and magnitude of the wind velocity. In Fig. 9, the full mass balance for the same case is shown, again with (left) and without (right) taking ice cover into account in the fetch calculation. In both Figs. 8 and 9, the largest difference between the two cases is seen between 6 and 8 days, when there is significantly more surface oil in the case where the fetch is calculated from the ice edge. This demonstrates the importance of taking the dynamically changing ice cover into account in calculating the wave field.

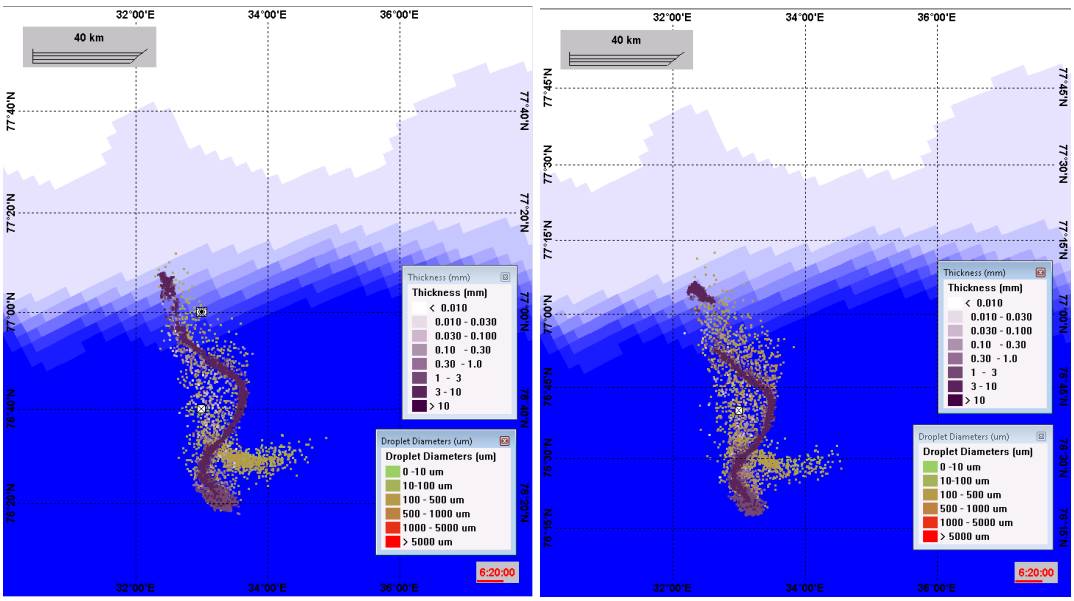

Figure 7 Overview of the case considered. Surface oil is shown in purple colours, submerged oil in brown-ish colours, and the ice cover is shown from full ice cover (white) to open water (blue). The release point is indicated by the white square. To the left, ice is taken into account in the fetch calculation, and to the right it is not. The time shown in the lower right corner corresponds to the time-axis in Fig. 8.

Nordam, T., E. Litzler, P. Ronningen, J. Aune, T.F. Hagelien, A. Luktu, C.J. Beegle-Krause, and U. Bronner, Oil Spill Contingency and Response Modelling in Ice-covered Waters, Proceedings of the Forty-first AMOP Technical Seminar, Environment and Climate Change Canada, Ottawa, ON, Canada, pp. 957-973, 2018.

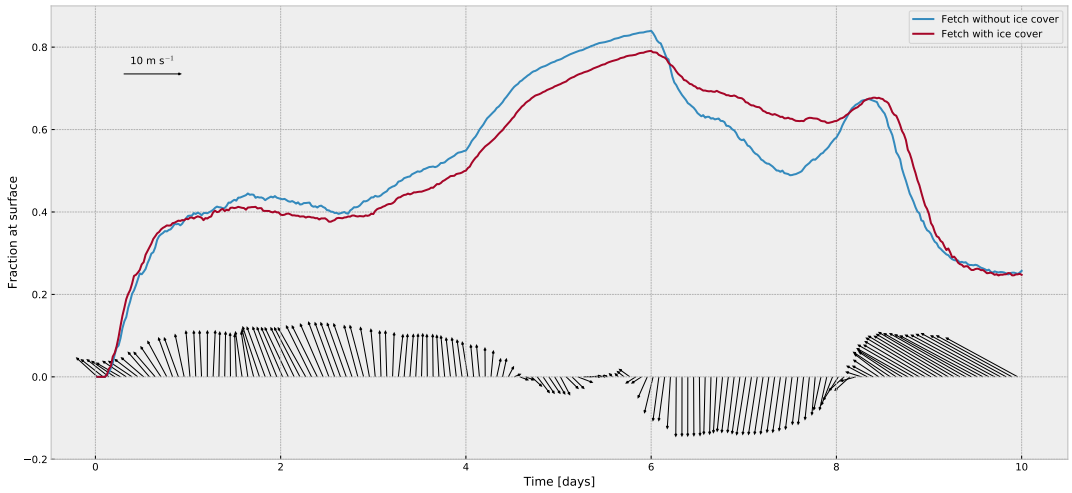

Figure 8 Mass of oil at the surface, as a fraction of the combined oil at the surface and in the water column. The wave state has been calculated both with and without taking ice cover into account in the fetch length. Additionally, the wind speed and direction is shown (up is north, right is east, etc.).

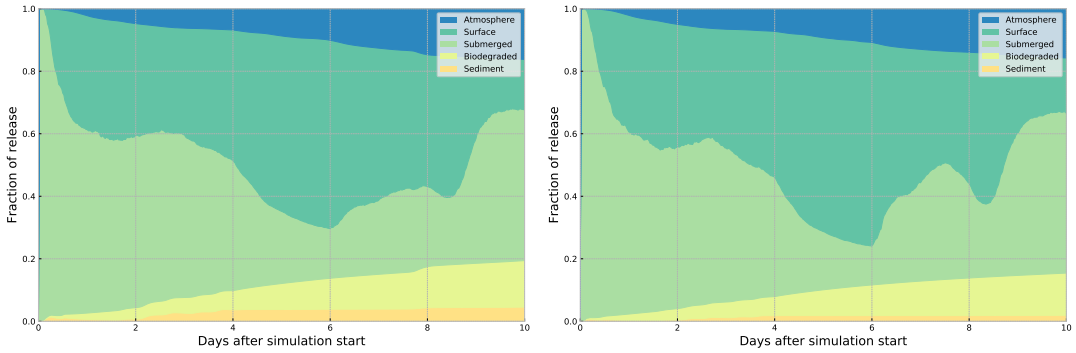

Figure 9 Mass balance with (left panel) or without (right panel) accounting for ice in the fetch calculation.

3.3 Ignitability

A hypothetical oil spill scenario is considered, where the oil is released in a blowout from a depth of about 200 meters, and surfaces almost directly above the release point. In Fig. 10, an example of a map showing the ignitability of surface oil is shown. In this case, the oil remains ignitable for about 8 hours. As previously mentioned, this prediction does not take thickness into account, as oil drifting in open water will usually be too thin to be ignited without increasing the thickness by some means (e.g. fire booms). Instead, the oil in the red area in Fig. 10 should be interpreted as being ignitable *if* it can be concentrated to sufficient thickness, thus indicating where one should focus the efforts of response vessels for *in-situ* burning.

If the oil is released in full or partial ice cover, or if it drifts into the ice shortly after being released, the oil can remain ignitable for much longer than in open water, due to reduced evaporation and water uptake (Brandvik and Faksness, 2009).

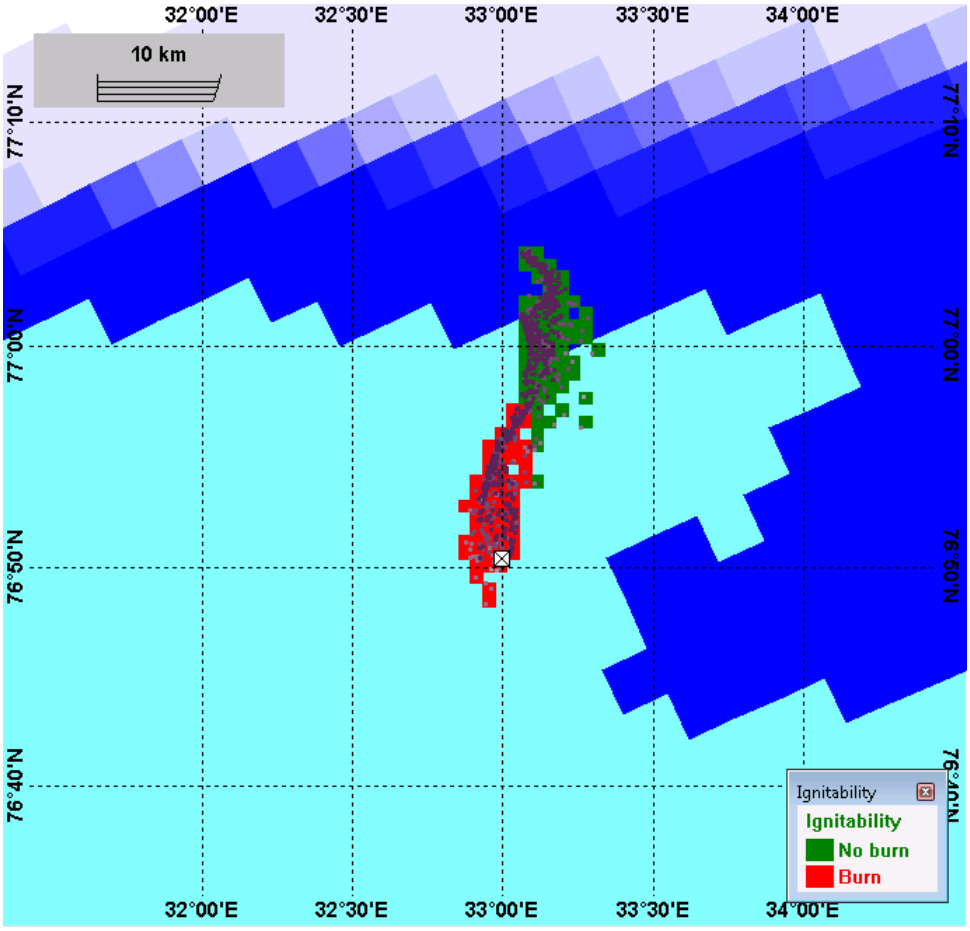

Figure 10 Ignitability of oil shown for an oil spill scenario. The red area contains ignitable oil.

4 Discussion and Conclusion

In this work, we have made several important improvements to OSCAR, to make it more suited for modelling of oil spills in cold and ice-covered waters. Additionally, the new scheme for vertical mixing and the calculation of ignitability of surface oil are both relevant improvements for oil spills at any location. With these new changes, OSCAR will give more realistic predictions for the transport and fate of oil, in particular when ice is present.

The use of ice velocity from external sources such as a coupled ice-ocean model is highly relevant for oil spills in ice, or in cases where oil is spilled in open water, and later reaches the ice edge. The impact of this particular change will vary with scenario, location, and the details of the ice-ocean model (for further details, see Nordam et al. (2018)). The effect will be particularly pronounced where the motion of the ice is strongly affected by other factors than the current and wind, which will be the case for fast ice, or in cases where the rheology in the ice model allows the transmission of long-range forces within the ice sheet. Being able to read ice data on the standard netCDF format, OSCAR is well posed to take advantage of any advances in sea ice modelling.

The new vertical mixing scheme, which is available as an option, takes stratification of the water column into account. It can be used with data from any ocean model that produces temperature and salinity as output. Changes in vertical mixing can have a large impact on the transport and fate of an oil spill, as oil at different depths will experience different currents, and can end up in very different locations. Another recent improvement to OSCAR is

the option to read vertical and horizontal diffusivity from netCDF files, in the same way as currents and ice data. This makes it straightforward to use diffusivities from hydrodynamic models, specialised turbulence models such as GOTM (Umlauf et al., 2005), or even measurements. With access to more accurate data on vertical mixing, OSCAR will provide more accurate predictions of rise times for submerged oil droplets in the water column.

It should be noted, however, that accurate modelling of vertical mixing (both for oil spills and other applications) is a difficult problem, on which more research is needed. Some care should be taken in using the eddy diffusivity output from an Eulerian ocean model in a Lagrangian particle simulation, as diffusivity in an Eulerian model may be artificially increased to improve the numerical stability. Nevertheless, it remains true that a good scheme for vertical mixing should take the effect of stratification into account. A strong, stable gradient can cause the diffusivity to drop by several orders of magnitude over a short distance (Gräwe et al., 2012), severely reducing the mixing of small droplets and dissolved components into deeper layers.

In conclusion, we continue to upgrade OSCAR to remain a state-of-the-art tool for contingency planning and environmental risk assessment for oil spills in cold and ice-covered waters.

5 Acknowledgements

The research described in this paper was funded by Equinor. The authors would like to thank their friends and colleagues Raymond Nepstad, Jørgen Skancke, Per Johan Brandvik and Øistein Johansen for many an interesting discussion in the SINTEF CoffeeLab.

6 References

ASCE, "State-of-the-art review of modeling transport and fate of oil spills", *Journal of Hydraulic Engineering*, 122:594–609, 1996.

Bagi, A., D. M. Pampanin, O. G. Brakstad, and R. Kommedal, "Estimation of hydrocarbon biodegradation rates in marine environments: A critical review of the Q10 approach", *Marine Environmental Research*, 89:83–90, 2013.

Beegle-Krause, C., "Chapter 9 - Challenges and Mysteries in Oil Spill Fate and Transport Modeling", in Stout, S. A. and Z. Wang, eds., *Oil Spill Environmental Forensics Case Studies*, Butterworth-Heinemann, pp. 187–199, 2018.

Brandvik, P. J. and L.-G. Faksness, "Weathering processes in Arctic oil spills: Meso-scale experiments with different ice conditions", *Cold Regions Science and Technology*, 55:160–166, 2009.

Brandvik, P. J., J. Fritt-Rasmussen, M. Reed, and N. R. Bodsberg, "Predicting ignitability for in situ burning of oil spills as a function of oil type and weathering degree", in *Proceedings of the 33rd AMOP Technical Seminar, Halifax, NS.*, Environment Canada, 2010, pp. 773–786.

Brandvik, P. J., O. Johansen, F. Leirvik, U. Farooq, and P. S. Daling, "Droplet Breakup in Subsurface Oil Releases – Part 1: Experimental Study of Droplet Breakup and Effectiveness of Dispersant Injection", *Marine Pollution Bulletin*, 73:319–326, 2013.

Carter, D., "Prediction of wave height and period for a constant wind velocity using the JONSWAP results", *Ocean Engineering*, 9:17–33, 1982.

Daling, P. S., P. J. Brandvik, D. Mackay, and Ø. Johansen, "Characterization of crude oils for environmental purposes", *Oil and Chemical Pollution*, 7:199–224, 1990.

Dee, D., S. Uppala, A. Simmons, P. Berrisford, P. Poli, S. Kobayashi, U. Andrae, M. Balmaseda, G. Balsamo, P. Bauer, et al., "The ERA-Interim Reanalysis: Configuration and Performance of the Data Assimilation System", *Quarterly Journal of the Royal Meteorological Society*, 137:553–597, 2011.

Egbert, G. D., A. F. Bennett, and M. G. Foreman, "TOPEX/POSEIDON tides estimated using a global inverse model", *Journal of Geophysical Research: Oceans*, 99:24821–24852, 1994.

El-Tahan, H., G. Comfort, and R. Abdelnour, "Development of a Methodology for Computing Oil Spill Motion in Ice-infested Waters", *Rep. submitted by Fleet Technology Limited, Kanata, Ont., to Atmospheric Environment Service, Downsview, Ont*, 1988.

Gräwe, U., E. Deleersnijder, S. H. A. M. Shah, and A. W. Heemink, "Why the Euler scheme in particle tracking is not enough: the shallow-sea pycnocline test case", *Ocean Dynamics*, 62:501–514, 2012.

Hibler III, W., "A Dynamic Thermodynamic Sea Ice Model", *Journal of Physical Oceanography*, 9:815–846, 1979.

Hunke, E. and J. Dukowicz, "An Elastic-viscous-plastic Model for Sea Ice Dynamics", *Journal of Physical Oceanography*, 27:1849–1867, 1997.

Ichiye, T., "Upper Ocean Boundary-Layer Flow Determined by Dye Diffusion", *The Physics of Fluids*, 10:S270–S277, 1967.

Johansen, Ø., "Numerical modelling of physical properties of weathered North Sea crude oils.", Tech. Rep. DIWO-report no. 15. IKU-report 02.0786.00/15/91, IKU, 1991.

Johansen, O., P. J. Brandvik, and U. Farooq, "Droplet Breakup in Subsea Oil Releases – Part 2: Predictions of Droplet Size Distributions With and Without Injection of Chemical Dispersants", *Marine Pollution Bulletin*, 73:327–335, 2013.

Johansen, Ø., M. Reed, and N. R. Bodsberg, "Natural dispersion revisited", *Marine pollution bulletin*, 93:20–26, 2015.

Johansen, O., H. Rye, and C. Cooper, "DeepSpill—Field Study of a Simulated Oil and Gas Blowout in Deep Water", *Spill Science & Technology Bulletin*, 8:433–443, 2003.

Lofthus, S., R. Netzer, A. S. Lewin, T. M. Heggeset, T. Haugen, and O. G. Brakstad, "Biodegradation of n-alkanes on oil–seawater interfaces at different temperatures and microbial communities associated with the degradation", *Biodegradation*, 29:141–157, 2018.

Millero, F. J. and A. Poisson, "International one-atmosphere equation of state of seawater", *Deep Sea Research Part A. Oceanographic Research Papers*, 28:625–629, 1981.

Nordam, T., C. Beegle-Krause, J. Skancke, R. Nepstad, and M. Reed, "Improving oil spill trajectory modelling in the Arctic", *Submitted to Marine Pollution Bulletin*, 2018.

Reed, M. and O. M. Aamo, "Real time oil spill forecasting during an experimental oil spill in the arctic ice", *Spill Science & Technology Bulletin*, 1:69–77, 1994.

Reed, M., P. Daling, O. Brakstad, I. Singsaas, L. Faksness, B. Hetland, and N. Ekrol, "OSCAR 2000: A Multi-Component 3-Dimensional Oil Spill Contingency and Response Model.", in *Proceedings of the 23rd AMOP Technical Seminar, Vancouver, BC.*, Environment Canada, 2000, pp. 663–680.

Rye, H., O. Johansen, I. Durgut, M. Reed, and M. K. Ditlevsen, "ERMS Report No. 21: Restitution of an impacted sediment", Tech. rep., SINTEF, 2006.

Simecek-Beatty, D., "Chapter 11 - Oil Spill Trajectory Forecasting Uncertainty and Emergency Response", in Fingas, M., ed., *Oil Spill Science and Technology*, Gulf Professional Publishing, Boston, pp. 275–299, 2011.

Slagstad, D. and T. A. McClimans, "Modeling the Ecosystem Dynamics of the Barents Sea Including the Marginal Ice Zone: I. Physical and Chemical Oceanography", *Journal of Marine Systems*, 58:1–18, 2005.

Smagorinsky, J., "General Circulation Experiments With the Primitive Equations: I. The Basic Experiment", *Monthly weather review*, 91:99–164, 1963.

Stewart, R. H., *Introduction to physical oceanography*, 2008, available electronically from http://hdl.handle.net/1969.1/160216.

Sundfjord, A., I. Ellingsen, D. Slagstad, and H. Svendsen, "Vertical mixing in the marginal ice zone of the northern Barents Sea—Results from numerical model experiments", *Deep Sea Research Part II: Topical Studies in Oceanography*, 55:2154–2168, 2008.

Umlauf, L., H. Burchard, and K. Bolding, *GOTM – Scientific Documentation: version 3.2*, Marine Science Reports, Leibniz-Institute for Baltic Sea Research, Warnemuende, Germany, 2005, please see up-to-date version on www.gotm.net.

US Army Corps Of Engineers, "Shore protection manual", Tech. rep., 1984.

Venkatesh, S., H. El-Tahan, G. Comfort, and R. Abdelnour, "Modelling the behaviour of oil spills in ice-infested waters", *Atmosphere-Ocean*, 28:303–329, 1990.